Identification and validation of a fatty acid metabolism gene signature for the promotion of metastasis in liver cancer

ZHENSHAN ZHANG[1,2*], JUN SUN[1*], CHAO JIN[3,4], LIKUN ZHANG[5], LEILEI WU[6] and GENDONG TIAN[1]

[1]Department of Hepatobiliary Surgery, The Second Hospital, Cheeloo College of Medicine, Shandong University, Jinan, Shandong 250033; [2]Department of Radiation Oncology, Shanghai Proton and Heavy Ion Center, Shanghai 201321; [3]Department of Ocean, Shandong University, Weihai, Shandong 264209; [4]Department of Pharmacy, Zhejiang Qianji Fang Pharmaceutical Technology Co., Ltd., Hangzhou, Zhejiang 311710; [5]Department of Clinical Medicine, Qiqihar Medical University, Qiqihar, Heilongjiang 161003; [6]Department of Radiation Oncology, Shanghai Pulmonary Hospital, Tongji University School of Medicine, Shanghai 200433, P.R. China

Received June 20, 2023; Accepted August 10, 2023

DOI: 10.3892/ol.2023.14044

Abstract. Metastasis is a fatal status for liver cancer, and the identification of an effective prediction model and promising therapeutic target is essential. Given the known relationship between fatty acid (FA) metabolism and the liver, the present study aimed to investigate dysregulation of genes associated with FA metabolism in liver cancer. Bioinformatics analyses were performed on data from patients with hepatocellular carcinoma (HCC) obtained from The Cancer Genome Atlas database using R software packages. Online public tools such as the Human Protein Atlas, Tumor Immune Single-Cell Hub and the University of Alabama at Birmingham Cancer Data Analysis portal were also utilized. Some essential results were further verified using *in vitro* experiments using HepG2 liver cancer cells. A signature consisting of three genes associated with the progression and prognosis of HCC and FA metabolism was identified. When samples were scored based on the expression of these genes and divided according to the median value, the higher score group showed a worse outcome and repressive immune microenvironment than the lower score group. Downstream pathways such as hypoxia, IL6/JAK/STAT3 and epithelial-mesenchymal transition were found to be significantly activated in the higher score group. As the core factor in the signature, mitochondrial ribosomal protein L35 (MRPL35) was found to be upregulated in HCC and to have certain impacts on the dysregulation of effective immunity. Further investigations and *in vitro* experiments indicated that MRPL35 facilitates the migration and invasion abilities of liver cancer, and the resistance of HCC to treatment. These findings have important implications regarding the characteristics and mechanisms of metastasis in liver cancer, and provide a promising signature based on FA metabolism-related genes that may be used to predict outcomes and explored as a novel therapeutic target in liver cancer.

Correspondence to: Professor Gendong Tian, Department of Hepatobiliary Surgery, The Second Hospital, Cheeloo College of Medicine, Shandong University, 247 Beiyuan Street, Jinan, Shandong 250033, P.R. China
E-mail: tiangendong@163.com

Dr Leilei Wu, Department of Radiation Oncology, Shanghai Pulmonary Hospital, Tongji University School of Medicine, 507 Zhengmin Road, Yangpu, Shanghai 200433, P.R. China
E-mail: wiley0916@126.com

*Contributed equally

Key words: MRPL35, liver cancer, hepatocellular carcinoma, metastasis, fatty acid metabolism

Introduction

Although the occurrence of liver cancer has declined for decades and has currently plateaued, it is still considered one of the most fatal cancers (1). Cancer statistics showed 906,000 new liver cancer cases and 830,000 deaths worldwide in 2020. The five-year net survival was reported as 5-30% during 2000-2014 (2).

Metastasis and recurrence present formidable obstacles to improving the long-term survival of patients with HCC. Currently, surgical intervention is the most effective approach for the treatment of HCC. However, when initially diagnosed with HCC, a considerable number of patients are already at an advanced stage, rendering them ineligible for curative surgery (3). Consequently, the acquisition of a comprehensive understanding of the mechanisms underlying HCC metastasis is of utmost importance for fostering the development of innovative therapeutic strategies aimed at improving patient outcomes.

Fatty acids (FAs) are energy storage substances that cells can utilize as a source of energy for growth and multiplication (4). To maintain rapid proliferation, the metabolic level of FA synthesis in cancerous cells is upregulated to meet the biosynthesis demands of membranes and signaling molecules (5,6). Consequently, metabolic dysregulation may

contribute to tumor initiation, development and progression (7,8). Also, the upregulation of FA metabolism occurs in HCC (9). There is preclinical and clinical evidence that FA-related genes participate in HCC development and prognosis (10,11). However, studies concerning the dysregulation of FA metabolism in HCC metastasis are rare. In addition to promoting HCC, upregulated FA metabolism has also been shown to impair the response of HCC to targeted therapies such as sorafenib (12) and bevacizumab (13). Furthermore, studies have suggested that high palmitic acid levels induce the upregulation of programmed cell death ligand-1 (14), and that the β-oxidation of FAs (15,16) and short-chain FAs (10,17) facilitates the activity of Treg cells and M2 macrophages, thereby impairing their antitumor immune efficacy.

The aim of the present study was to analyze the association between HCC metastasis and FA metabolism-related genes, and then to explore the value of the FA genetic signature in prognosis and as a novel therapeutic target. The findings may improve our understanding of HCC and help to optimize strategies for its treatment.

Materials and methods

Data acquisition. The expression arrays and associated clinical information of patients with HCC from The Cancer Genome Atlas (TCGA) were obtained via the University of California Santa Cruz Xena tool (http://xena.ucsc.edu/) (18) for subsequent analysis. After excluding samples with no clear clinical information and OS <30 days, a total of 362 patients participated. The Human Protein Atlas portal (https://www.proteinatlas.org/) was searched to acquire images of HCC and adjacent normal tissue immunohistochemistry (IHC) to show dysregulation of a key gene at the protein level. The gene set for FA metabolism was obtained from the Molecular Signatures Database (MSigDB) (19,20). After entering 'fatty' in the keywords box with the filter of *Homo sapiens*, a total of 187 gene sets were obtained. The target gene set comprised genes from the FA metabolism gene sets that overlapped with gene sets associated with metastasis and worse OS risk. Kaplan-Meier survival curve analysis was conducted using the Gene Expression Profiling Interaction Analysis 2 web application (http://gepia2.cancer-pku.cn/#index) to explore the association of specific genes with OS in HCC. The University of Alabama at Birmingham Cancer Data Analysis (UALCAN) portal (http://ualcan.path.uab.edu/) was utilized to analyze the correlation between promoter methylation level and protein level of the key gene mitochondrial ribosomal protein L35 (MRPL35) and clinical status. UALCAN (ualcan.path.uab.edu/analysis-prot.html) was used to analyze the association between protein level and clinical characteristics from the Clinical Proteomic Tumor Analysis Consortium (CPTAC). TNMplot (https://tnmplot.com/analysis/) (21) public database was used to explore the relationship between MRPL35 and metastatic status in HCC.

Construction of a co-expression network and exploration of the association between gene modules and metastatic status. The workflow of the present study is shown in Fig. 1. Following the acquisition of the RNA-sequencing (RNA-seq) array and clinical information of patients with HCC, a weighted correlation network analysis (WGCNA) (22) was conducted using R (Vision: 3.6.3; r-project.org/). WGCNA was performed to investigate the association between gene modules and clinical variables (age, T stage, N stage and M stage). In this analysis, gene significance (GS) was determined by taking the logarithm (base 10) of the P-value resulting from the linear regression analysis conducted on gene expression and clinical features. Module significance (MS) was defined as the mean GS across all genes within a module. The module exhibiting the highest absolute MS among all the modules selected for a specific clinical feature was considered to be associated with that feature. To condense the expression patterns of all genes within a module, a singular representative expression value known as the module eigengene (ME) was calculated, which served as the primary component in the principal component analysis. By evaluating the associations between MEs and clinical features, the most pertinent gene module for each clinical feature of interest was identified. Further analysis was conducted on the module displaying the strongest association with the desired clinical features.

Functional enrichment analysis. A combined WGCNA and FA (WF) score was calculated by multiplying the expression value of each gene by the sum of its respective coefficients. The coefficients calculated by Least Absolute Shrinkage and Selection Operator (LASSO) (23) were as follows: CYP2S1, 0.043; MRPL35, 0.178; and PLCD3, 0.061. The HCC cohort was divided into high and low WF score groups according to the median WF score. Gene Set Enrichment Analysis (GSEA; gsea-msigdb.org/gsea/index.jsp) (19) was utilized to investigate the biological functions that differed between the two groups. The GSEA employed a cut-off threshold of nominal $P<0.05$ and a false discovery rate (FDR) <0.25. The LinkedOmics (https://www.linkedomics.org/admin.php) (24) online tool was used to analyze the potential function of MRPL35 in HCC.

LASSO Cox regression modeling and survival analysis. Cox regression modeling using LASSO was performed with the LASSO-Cox regression tool available in Sangerbox (25) to select the most relevant genes. LASSO regression is characterized by variable selection and complexity regularization while fitting a generalized linear model. Therefore, regardless of whether the target dependent variable is continuous or discrete, LASSO regression is used to model and predict. COX survival analysis was conducted by glmnet, survival and survminer packages of R based on clinical information.

Analysis of immune cell infiltration. The differential infiltration of immune cells was assessed using the CIBERSORT algorithm (https://cibersortx.stanford.edu) (26). In this analysis, the default signature matrix comprising 1,000 permutations was employed. To enhance the reliability of the findings, only data with deconvolution $P<0.05$ were retained. Wilcoxon rank-sum test and signed-rank test were utilized appropriately to analyze the differences between clusters and in immune cell infiltration between the high and low WF score groups.

To assess the association between MRPL35 expression and immune infiltration, the TIMER2.0 (timer.comp-genomics.org/) (27) systematic platform was used to examine immunological attributes of cancer in TCGA data.

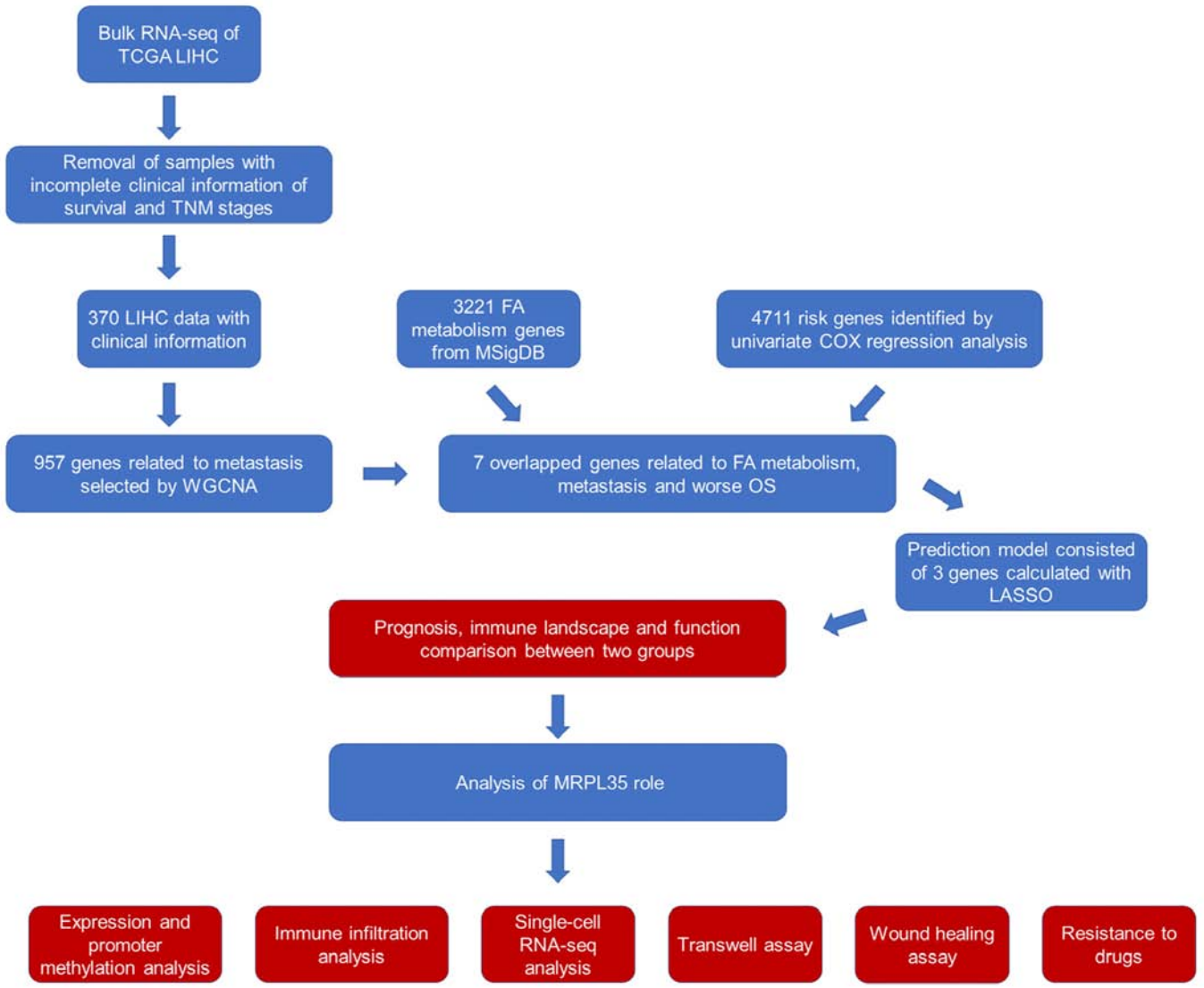

Figure 1. Flow chart of the study. RNA-Seq, RNA-sequencing; TCGA, The Cancer Genome Atlas; LIHC, liver hepatocellular carcinoma; WGCNA, weighted correlation network analysis; FA, fatty acid; MSigDB, Molecular Signatures Database; OS, overall survival; LASSO, Least Absolute Shrinkage and Selection Operator; MRPL35, mitochondrial ribosomal protein L35.

Validation of single-cell RNAseq (scRNA-seq). Tumor Immune Single-Cell Hub (tisch.comp-genomics.org/home/) (TISCH) is a public source of scRNA-seq data on the tumor microenvironment (TME). TISCH collected a total of 76 sets of high-quality tumor single-cell transcriptome data from GEO and ArrayExpress and corresponding patient information, covering 27 cancer types. It provides specific annotation of cell type at a single-cell level and allows gene expression in the TME to be investigated (28).

Cell line and culture. The HepG2 liver cancer cell line (identified by Short Tandem repeat) was purchased from The Cell Bank of Type Culture Collection of The Chinese Academy of Sciences. The cells were cultured at 37˚C in a humid atmosphere with 5% CO_2 and maintained in Dulbecco's modified Eagle's medium (DMEM; Gibco; Thermo Fisher Scientific, Inc.) supplemented with 10% fetal bovine serum (FBS; Gibco; Thermo Fisher Scientific, Inc.), 100 U/ml penicillin and 100 μg/ml streptomycin (Beijing Solarbio Science & Technology Co., Ltd.).

Small interfering RNA (siRNA) and reverse transcription-quantitative PCR (RT-qPCR). Two siRNAs targeting MRPL35 (siMRPL35-1 and siMRPL35-2) and a control siRNA (siCtrl) were synthesized and designed by Sangon Biotech Co., Ltd. to suppress the expression of MRPL35 in HepG2 cells. To initiate transfection, cells were plated in 6-well plates at a density of $1x10^5$ cells/well and incubated at 37˚C until 70% confluency was reached. Subsequently, Lipofectamine® 3000 (Invitrogen; Thermo Fisher Scientific, Inc.) was used to transfect the cells with siRNAs or siCtrl (<60 nM, following the protocols provided by the manufacturer at room temperature for 20 min. The antisense sequences of the three siRNAs were as follows: siMRPL35-1, TAGTCATATTCAGACACCAGTTGTT; siMRPL35-2, CAACTGTGTCAAGAATGCCTCTCTT; and siCtrl, TAGATACTTAGACACGACTTTCGTT.

To confirm the efficacy of siRNA transfection, RT-qPCR was utilized to detect the level of MRPL35 after transfection. Following 36 h incubation under 37˚C, total RNA was isolated from cells using TRIzol® (Invitrogen; Thermo Fisher Scientific, Inc.). Subsequently, cDNA synthesis was performed

using a RevertAid First Strand cDNA Synthesis kit (Thermo Fisher Scientific, Inc.) according to the manufacturer's protocols. RT-qPCR was performed using iQ™ SYBR Green Supermix (Bio-Rad Laboratories, Inc.). The following primers were employed for the qPCR analysis: MRPL35 forward, 5'-TTGGCATCTTCAACCTACCGC-3' and reverse, 5'-GGAGGAAACAACTGGTGTCTGA-3'; GAPDH forward, 5'-ACAACTTTGGTATCGTGGAAGG-3' and reverse, 5'-GCCATCACGCCACAGTTTC-3' and the thermocycling condition was 94˚C 60sec, 37˚C 60 sec, 72˚C for 120 sec and 20-30 cycles. To calculate the relative expression level of the target gene, the $2^{-\Delta\Delta Cq}$ method was employed (29).

Wound healing assay. In the wound healing assay, HepG2 cells were seeded into a 6-well plate and allowed to reach 80% confluence. Under the deprivation of serum the cell monolayer was then scratched using a sterile micropipette tip. The floating cells were washed away with PBS to clear away any debris. Time points of 0, 12 and 24 h were chosen to observe the progression of wound healing within the gap with light microscope. Triplicate wells were examined for each condition to ensure reliability and reproducibility. The migration and closure of the wound were assessed by measuring the width of the wound at the two time points with those at 0 h.

Transwell assay. The Transwell assay, also known as the Boyden chamber assay, is a widely used technique for the study of cell migration and invasion. In this assay, Transwell chambers were prepared, each comprising an insert with 8-μm pores. The upper side of the membrane in the Transwell chamber was coated with a diluted Matrigel matrix in a 37˚C incubator for 30 min. Prior to the assay, the HepG2 cells were cultured in 2% FBS-DMEM for 12 h to induce starvation. The cells were then suspended in FBS-free DMEM and added to the upper chamber of the Transwell chamber at a concentration of $1x10^5$ cells/chamber. Simultaneously, DMEM supplemented with 10% FBS was added to the lower compartment. The Transwell chambers were then incubated for 48 h at 37˚C. Cells that had migrated to the lower surface of the filter membrane were fixed with 4% paraformaldehyde (20 min at room temperature) and stained with 0.5% crystal violet (10 min at room temperature). Cells remaining on the upper surface of the filter membrane were gently scraped off with a cotton swab. The lower surfaces of the membrane were then observed and images captured using an inverted light microscope, and the counting process was repeated three times.

MRPL35 and drug response. Drug Response CellMiner (https://discover.nci.nih.gov/cellminer/) is as an integration platform for both molecular and pharmacological data concerning the NCI-60 cancer cell lines (30). This resource was employed to explore the correlation between MRPL35 expression and drug response.

Statistical analysis. Statistical analyses were performed using the aforementioned online databases and R software (version 3.6.3). Data are presented as mean ± SD. For the statistical analysis of experimental data, GraphPad Prism 9.0 (GraphPad Software; Dotmatics) was employed. Unpaired Student's t and Wilcoxon rank-sum test and one-way ANOVA tests (with LSD as post hoc test) were used to calculate the significance of differences in data between and among groups. $P<0.05$ was considered to indicate a statistically significant result.

Results

Identification of the core gene set associated with HCC progression. Following the extraction of gene expression data and clinical information associated with HCC from TGCA, data on 362 cancerous samples with total prognostic information and 50 normal samples were obtained. These data were subjected to pre-processing cleanup and quality control prior to being subjected to WGCNA to investigate the associations between gene clusters and clinical characteristics associated with HCC. Based on scale-free topology, a soft-thresholding power of $\beta=4$ was chosen, indicating the reliability of the chosen power value. The rationality test yielded positive results as shown in Fig. S1A-C and following the identification of 44 gene modules (Fig. S1D), the skyblue3 and purple modules were found to exhibit significantly positive connections with M stage (cor=0.86, $P<0.05$) and N stage (cor=0.89, $P<0.05$) (Fig. S1E and F). As a result, the two modules, consisting of 957 genes, were recognized as the modules most relevant to tumor-distant metastasis and lymph node metastasis in HCC.

Consolidation of the gene set for prognosis prediction. There were seven genes in the area of overlap of the metastasis-associated WGCNA genes with the FA metabolism-related genes from MSigDB, and genes identified to be associated with the risk of HCC progression and OS by univariate Cox regression analysis (Fig. 2A). The LASSO-Cox regression model was used to further screen the seven core genes in HCC prognosis, and three genes were identified as preferable parameters (Fig. 2B and C). The relationship between the levels of the three genes, namely phospholipase C d3 (PLCD3), MRPL35 and cytochrome P450 family 2 subfamily S member 1 (CYP2S1), and outcomes is shown in Fig. 2D. A significant difference in OS was observed between the high and low WF score groups by Kaplan-Meier analysis ($P=0.009$; Fig. 2E).

The univariate Cox regression analysis of the seven genes is shown in Fig. 3A, each with $P<0.05$ and hazard ratio (HR)>1 for OS. MRPL35 had the highest HR among the three genes of particular interest (HR=1.461, $P<0.05$). Survival analyses were also conducted for the three preferred genes, CYP2S1 (HR=1.5, $P=0.024$, Fig. 3B), PLCD3 (HR=1.4, $P=0.042$, Fig. 3C and MRPL35 (HR=1.9, $P<0.001$, Fig. 3D). Subsequent expression analysis further indicated that PLCD3 and MRPL35 were significantly upregulated in cancerous samples compared with normal tissue ($P<0.05$; Fig. 3E-G).

These results indicate that the analysis of samples based on PLCD3, MRPL35 and CYP2S1 expression may be utilized to predict the OS of HCC. Therefore, the mechanism underlying the difference is worthy of exploration.

Immune infiltration and functional enrichment analysis. The effective infiltration of lymphocytes and ability of tumor cells to escape them affects the antitumor efficacy of immunity and the outcome of patients. With the CIBERSORT algorithm, the immune cells in the microenvironment of each sample were analyzed and predicted (Fig. 4A). In the high WF score group,

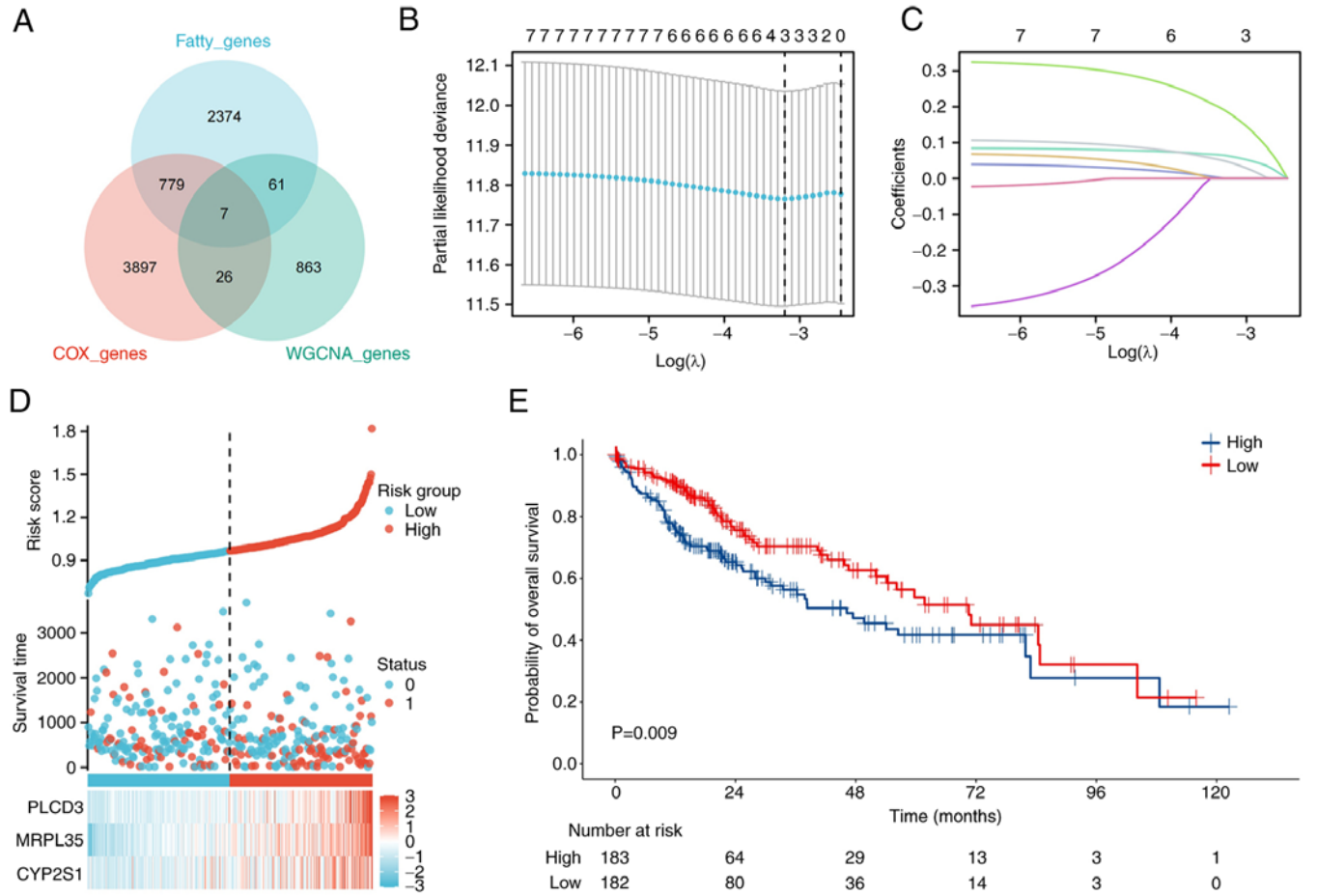

Figure 2. Consolidation of the predictive model. (A) Seven genes from the WGCNA, fatty acid metabolism-related and OS risk gene datasets overlapped in HCC. (B) LASSO analysis was conducted based on the seven genes, and three key genes were identified. (C) Dynamic screening process of variable coefficients. (D) Relationship between the expression levels of the three genes and the clinical status of patients with HCC. (E) Based on the WF scores calculated by LASSO, a worse outcome was observed in the group with high WF scores. WGCNA, weighted correlation network analysis; OS, overall survival; HCC, hepatocellular carcinoma; LASSO, Least Absolute Shrinkage and Selection Operator; WF, WGCNA and fatty acid; PLCD3, phospholipase C d3; MRPL35, mitochondrial ribosomal protein L35; CYP2S1, cytochrome P450 family 2 subfamily S member 1.

it was predicted that the infiltration of lymphocytes was lower (P=0.0014) and the infiltration of macrophages was higher (P=0.047) than that in the low WF score group (Fig. 4B). The specific types of immune cell were analyzed, which indicated the presence of more M0 macrophages and fewer $CD8^+$ T cells in the high WF score group compared with the low WF score group (P<0.05; Fig. 4C). The impaired immune efficacy might be a reason for the worse outcome of patients with a high WF score.

To investigate the downstream pathways and characteristics, GSEA was performed for the high and low WF score groups, which demonstrated that several tumor promotive pathways were evidently activated, namely TGF-β signaling, hypoxia, KRAS signaling, IL6/JAK/STAT3 signaling, epithelial-mesenchymal transition (EMT) and G2M checkpoint pathways, each with FDR <0.25 and normalized enrichment score >0 (Fig. 5). These pathways are known to promote tumor development and immune dysfunction.

Dysregulation of MRPL35 in HCC. Given the clinical value and potential mechanism based on the WF score, focus was given to the MRPL35 gene, which had the highest HR value, based on the assumption that it is the main factor facilitating tumor progression. In agreement with its mRNA level, the protein level of MRPL35 in HCC tumor tissue was higher than that in normal tissue (Fig. 6A), and a significant association with metastasis status was identified using TNMplot (P<0.05, Fig. 6B). Hypermethylation of a gene promoter region is known to regulate transcriptional silencing, and promoter hypomethylation can result in the upregulation of downstream genes. The analysis performed in the present study found that the promoter methylation levels of MRPL35 in HCC were significantly lower compared with those in tumor samples (P<0.05, Fig. 6C).

Downstream function and association with clinical characteristics of MRPL35 in HCC. LinkedOmics analysis was performed to evaluate the potential biological function of elevated MRPL35, and the results included activation of 'citrate cycle (TCA cycle)' and 'fatty acid metabolism' (Fig. S2A and B).

The associations of MRPL35 with clinical characteristics are shown in Fig. S2C-G. The results indicate that the level of MRPL35 was significantly higher in cases with residual tumor status R1 (vs. R0; Fig. S2E) and female patients (Fig. S2G), both P<0.05.

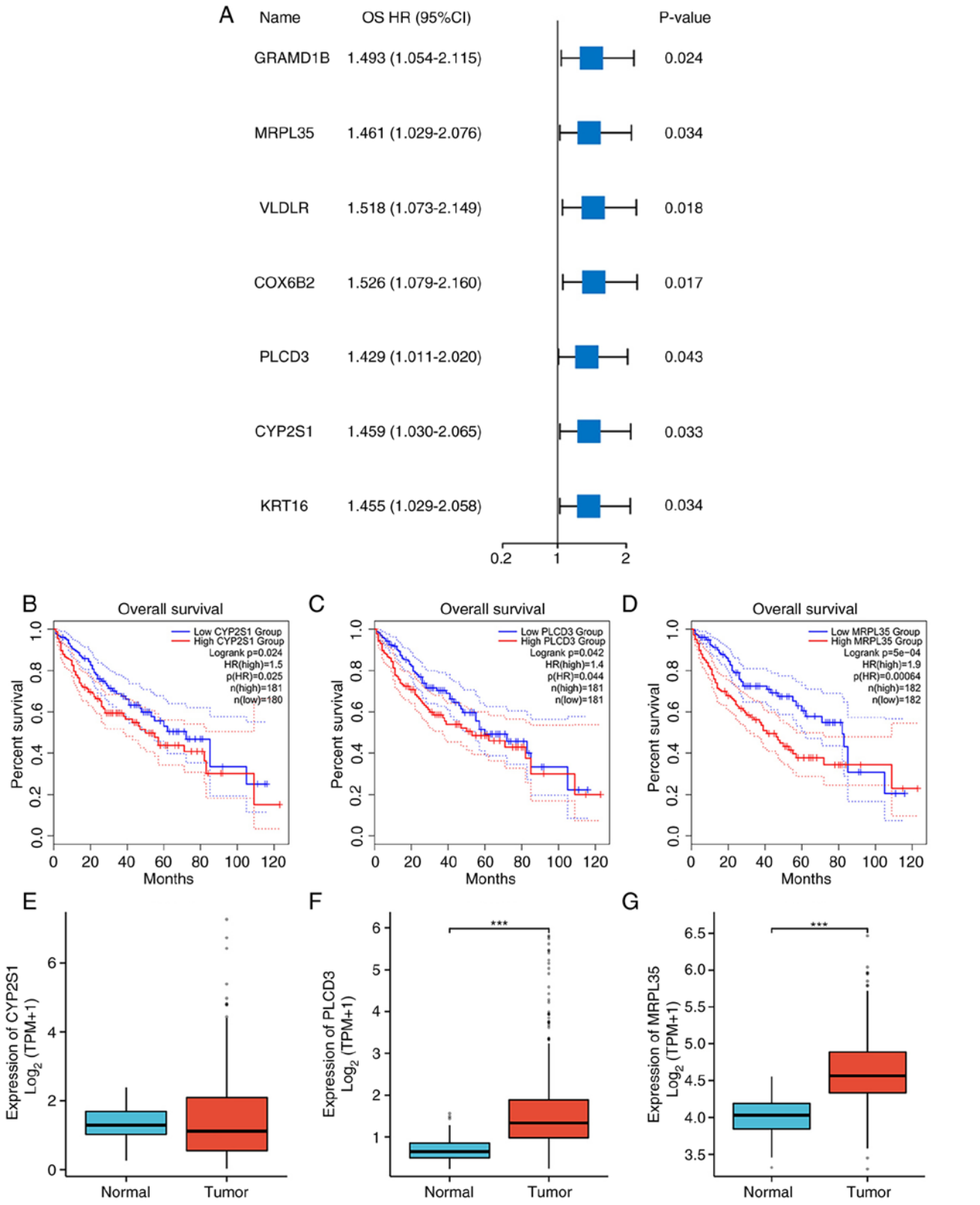

Figure 3. Survival and expression analysis. (A) Forest plot showing the OS HR and P-value of seven genes. OS analysis of (B) CYP2S1, (C) PLCD3 and (D) MRPL35 in HCC. Expression levels of (E) CYP2S1, (F) PLCD3 and (G) MRPL35 in normal and HCC tumor samples. ***P<0.001. OS, overall survival; HR, hazard ratio; CYP2S1, cytochrome P450 family 2 subfamily S member 1; PLCD3, phospholipase C d3; MRPL35, mitochondrial ribosomal protein L35; HCC, hepatocellular carcinoma; GRAMD1B, GRAM domain containing 1B; VLDLR, very low density lipoprotein; COX6B2, cytochrome C oxidase subunit 6B2; KRT16, keratin 16; TPM, transcripts per million.

Validation of scRNA-seq and infiltration analysis. When considering whether a gene possesses value as a therapeutic target or predictive parameter, the precise location of the gene at the cell level is important. The scRNA-seq method allows the expression level of a gene to be explored among different types of cells. In the microenvironment of HCC, MRPL35 was found to be mainly

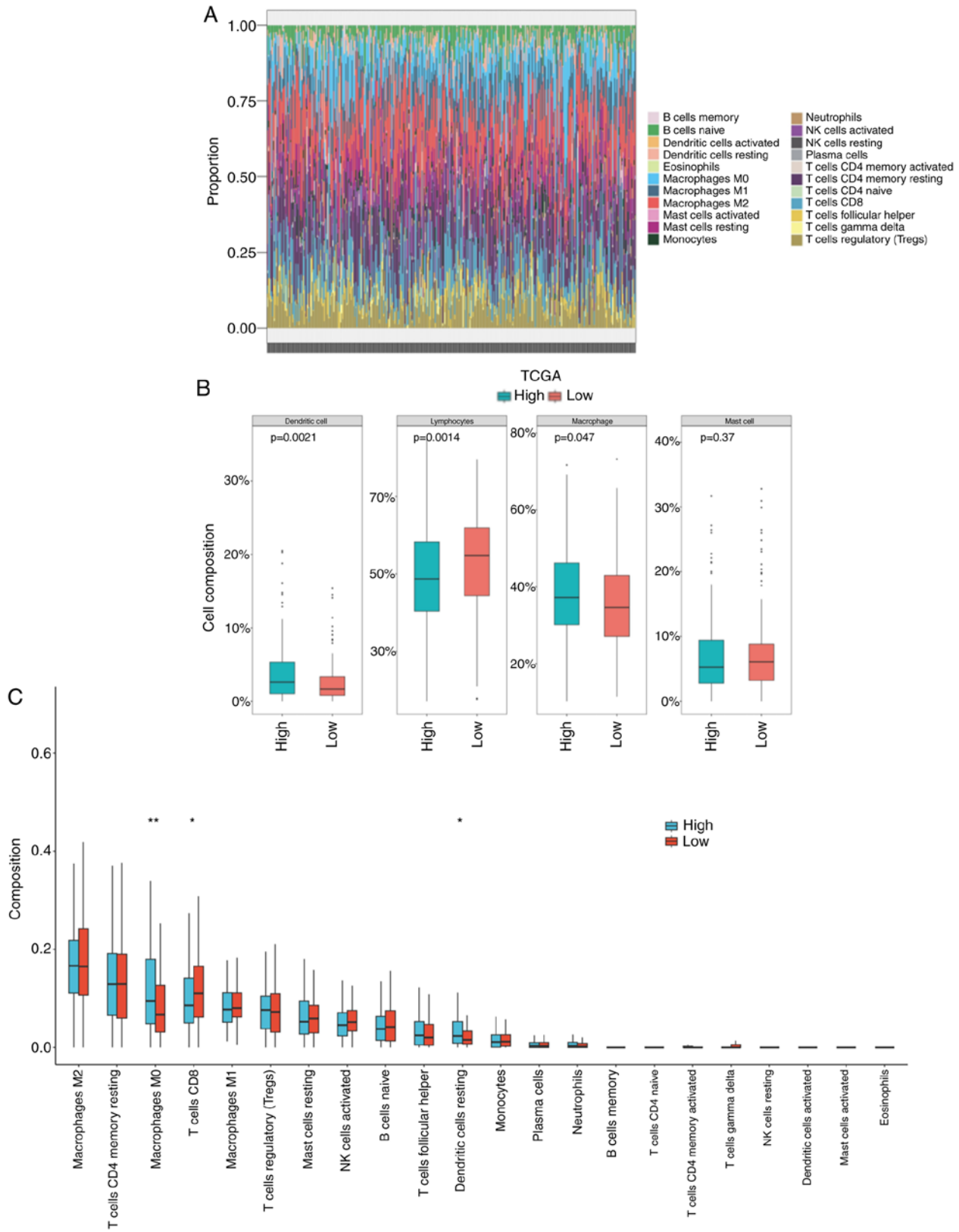

Figure 4. Immune function analysis. (A) Landscape of immune cells in 370 TCGA hepatocellular carcinoma samples. (B) Comparison of dendritic cell, lymphocyte, macrophage and mast cell compositions between high and low WF score groups (C). CIBERSORT analysis showing the difference in immune cell composition between high and low WF score groups *P<0.05, **P<0.01. TCGA, The Cancer Genome Atlas; WF, weighted correlation network analysis and fatty acid; NK, natural killer.

expressed by proliferating T cells and malignant cells (Fig. 6D). Similarly, a negative association with $CD8^{+}$ T cells and positive association with myeloid-derived suppressor cells (MDSCs) were observed in HCC (Fig. 6E). Furthermore, the comparison of MRPL35 IHC between tumor and normal human tissues supported the oncogenic role of MRPL3 (Fig. 6F-I).

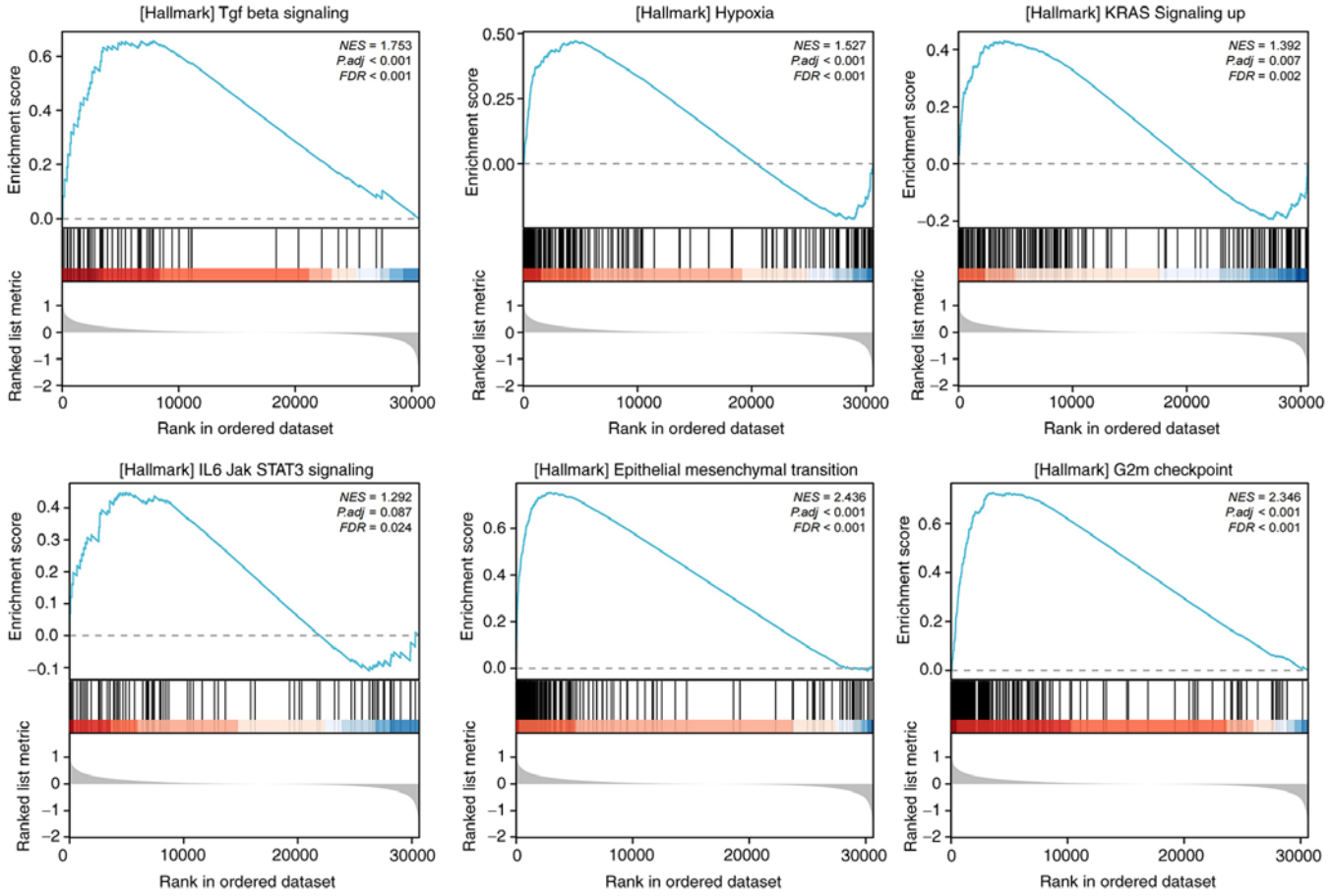

Figure 5. Functional enrichment of pathways. Gene set enrichment analysis revealed significantly activated pathways in the high WF score group compared with the low WF score group for TGF-β, hypoxia, KRAS, IL6/JAK/STAT3 signaling, epithelial-mesenchymal transition and G2M checkpoint pathways. WF, weighted correlation network analysis and fatty acid; NES, normalized enrichment score; P.adj, adjusted P-value; FDR, false discovery rate.

The aforementioned findings suggest that inhibiting the expression of MRPL35 in tumor cells may impair their proliferation, migration and immune-escape abilities.

Validation via in vitro experiments. To validate the role of MRPL35 as a risk factor and its potential as a novel therapeutic target, assays were conducted to evaluate the effect of its knockdown on the invasion and migration competence of HepG2 cells. Following the confirmation of the efficacy of knockdown by the MRPL35 siRNA compared with the siCtrl (P<0.001; Fig. 7A), negative control (NC), siCtrl and MRPL35 siRNA groups were evaluated *in vitro*. In the Transwell assay, the two siRNAs against MRPL35 showed a significant inhibitory effect on invasion after 48 h compared with siCtrl (P<0.001; Fig. 7B and C). In addition, the wound healing assay indicated that liver cancer cells with MRPL35 knockdown possessed significantly impaired ability to migrate compared with the controls (P<0.001; Fig. 7D and E). These experimental results suggest that MRPL35 may contribute to liver cancer metastasis and the blockade of MRPL35 could be a promising therapeutic target.

Correlation between the response to drugs and MRPL35 levels. To investigate the potential value of MRPL35 in drug treatment, an analysis of the correlation between the expression of MRPL35 and the response to the drug in 60 cell lines was conducted. The results indicated that MRPL35 was negatively correlated with the IC_{50} of 10 in 16 drugs: LY-3023414, Everolimus, spebrutinib, PQR-620, JNJ-42756493, M2698, INK-128, Rapamycin, futibutinib and WORTMANNIN, all with a correlation coefficient <0 and P<0.05 (Fig. 8). This provides preliminary guidance for strategies that may be applicable to patients with high MRPL35 levels.

Discussion

The occurrence of metastasis is a fatal sign for patients with HCC as it indicates the loss of opportunity to receive surgical treatment (3). Therefore, studies of biomarkers and promising therapeutic target are required.

Given the tight physiological and pathological relationship between FA metabolism and the liver (31), the clinical value of FA metabolism-related genes in HCC was explored in the present study. WGCNA identified 957 genes that may be promotive for HCC metastasis, from which seven were identified to have an association with FA metabolism and OS. After filtering using the LASSO algorithm, three core genes remained: PLCD3, MRPL35 and CYP2S1. Studies have reported the tumor-promotive role of PLCD3 in thyroid cancer (32) and osteosarcoma (33), the role of MRPL35 in gastric (34) and colorectal (35) cancer, and the role of CYP2S1 in breast (36) and lung (37) cancer. Consistent with

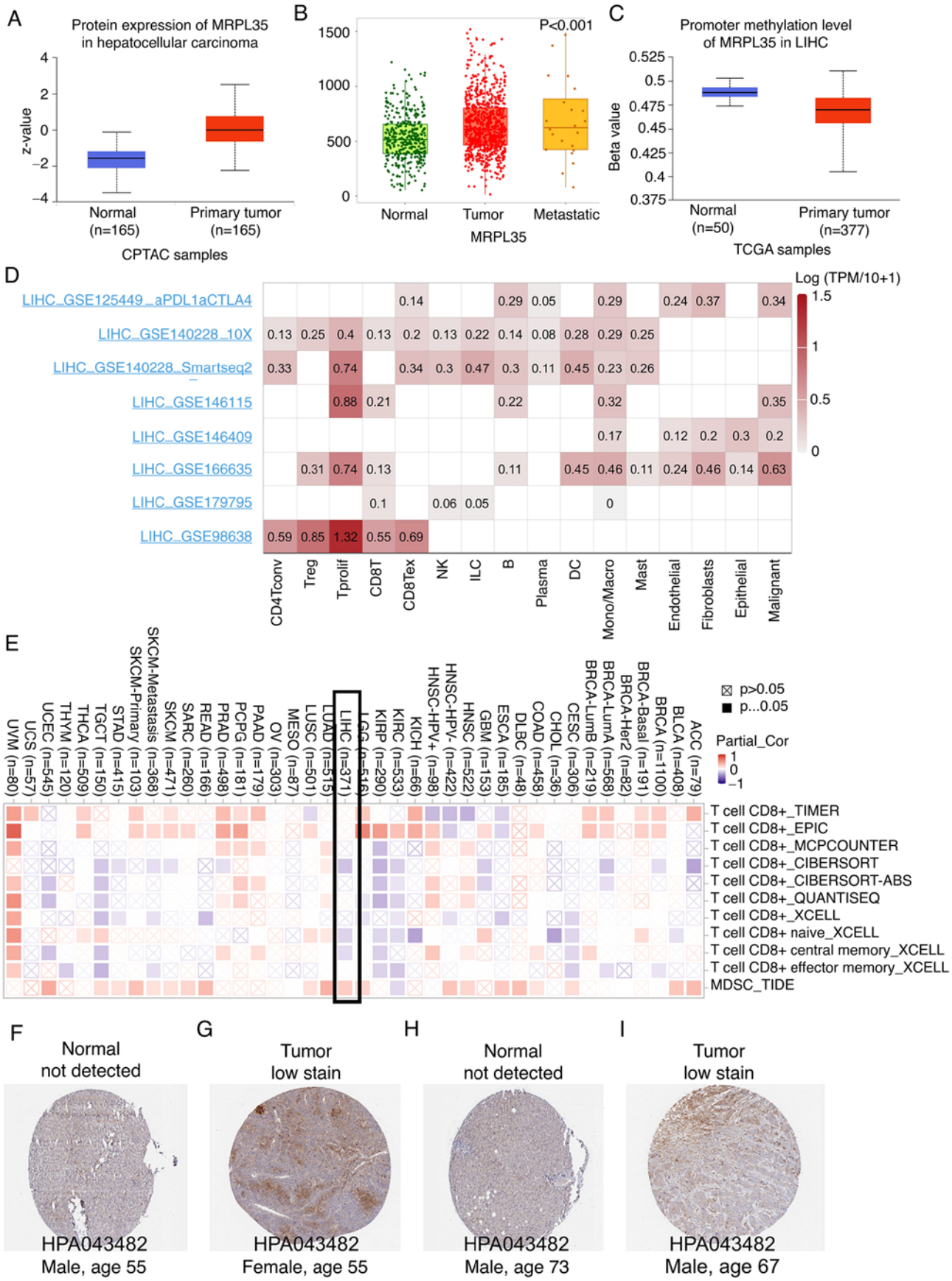

Figure 6. Analysis of the expression of MRPL35 and its association with immunity. (A) Protein level of MRPL35 in normal and HCC tumor samples. (B) Association between MRPL35 expression and HCC progression. (C) Comparison of promoter methylation level of MRPL35 between normal and LIHC samples. (D) Single cell RNA-sequencing analysis of MRPL35 in HCC. (E) Investigation of the correlation between MRPL35 expression level and the counts of $CD8^+$ T cells and MDSCs. (F-I) Validation of the expression of MRPL35 in (F,H) normal tissues and (G,I) HCC tumor tissues shown in immunohistochemical staining images from the Human Protein Atlas. MRPL35, mitochondrial ribosomal protein L35; HCC, hepatocellular carcinoma; LIHC, liver HCC; MDSCs, myeloid-derived suppressor cells; CPTAC, Clinical Proteomic Tumor Analysis Consortium; TCGA, The Cancer Genome Atlas; TPM, transcripts per million.

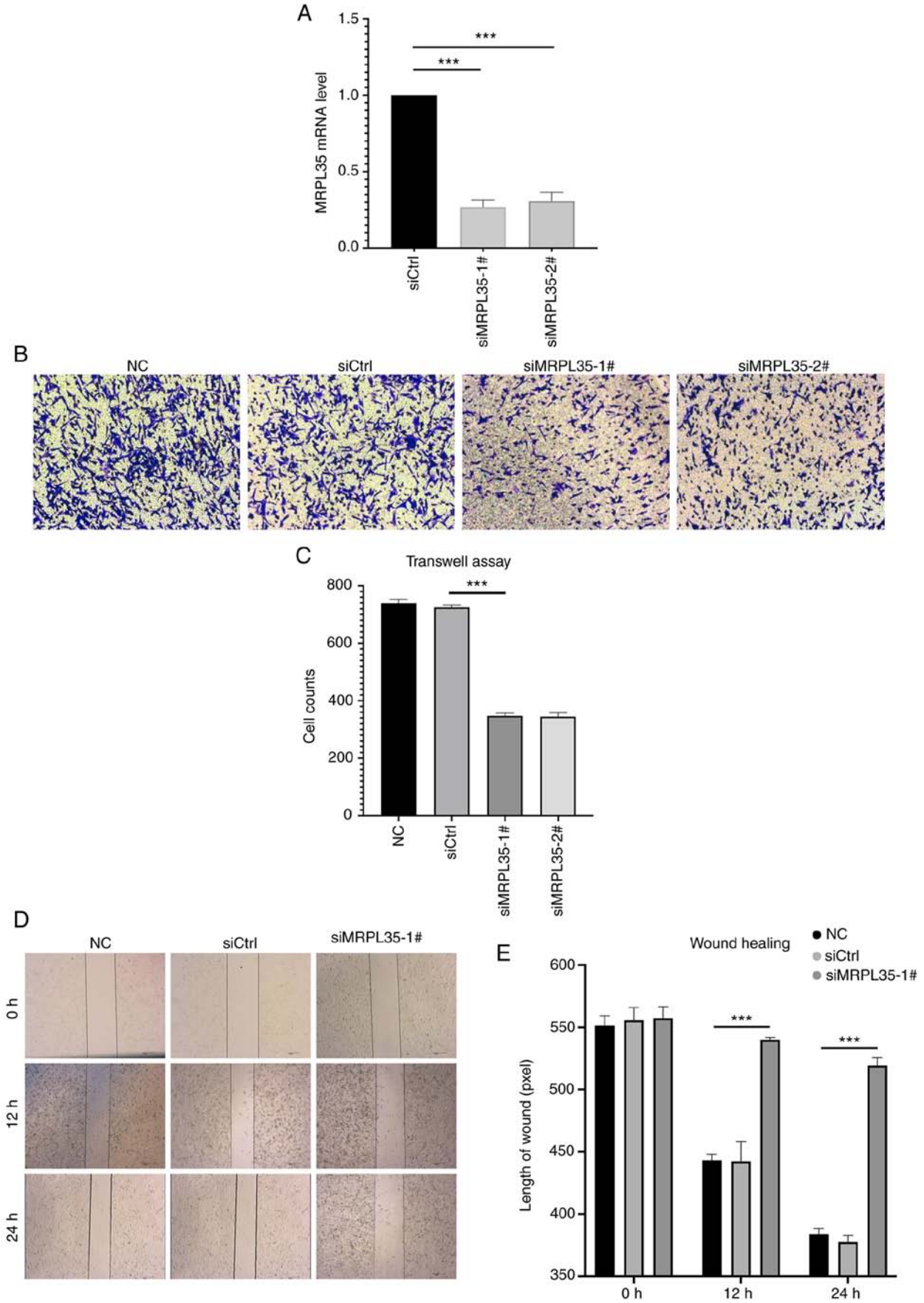

Figure 7. *In vitro* experiments on the role of MRPL35 in HepG2 liver cancer cells. (A) Reverse transcription-quantitative PCR analysis showed that two siRNAs targeting MRPL35 were effective in decreasing MRPL35 expression levels in the cells. (B) Representative images and (C) quantified data from a Transwell assay showing that MRPL35 knockdown significantly reduced the invasion ability of the HepG2 cells. (D) Representative wound assay images and (E) quantified data showing that MRPL35 knockdown significantly reduced the migration ability of the HepG2 cells. ***P<0.001. MRPL35, mitochondrial ribosomal protein L35; si, small interfering; NC, negative control (untransfected cells); siCtrl, si control.

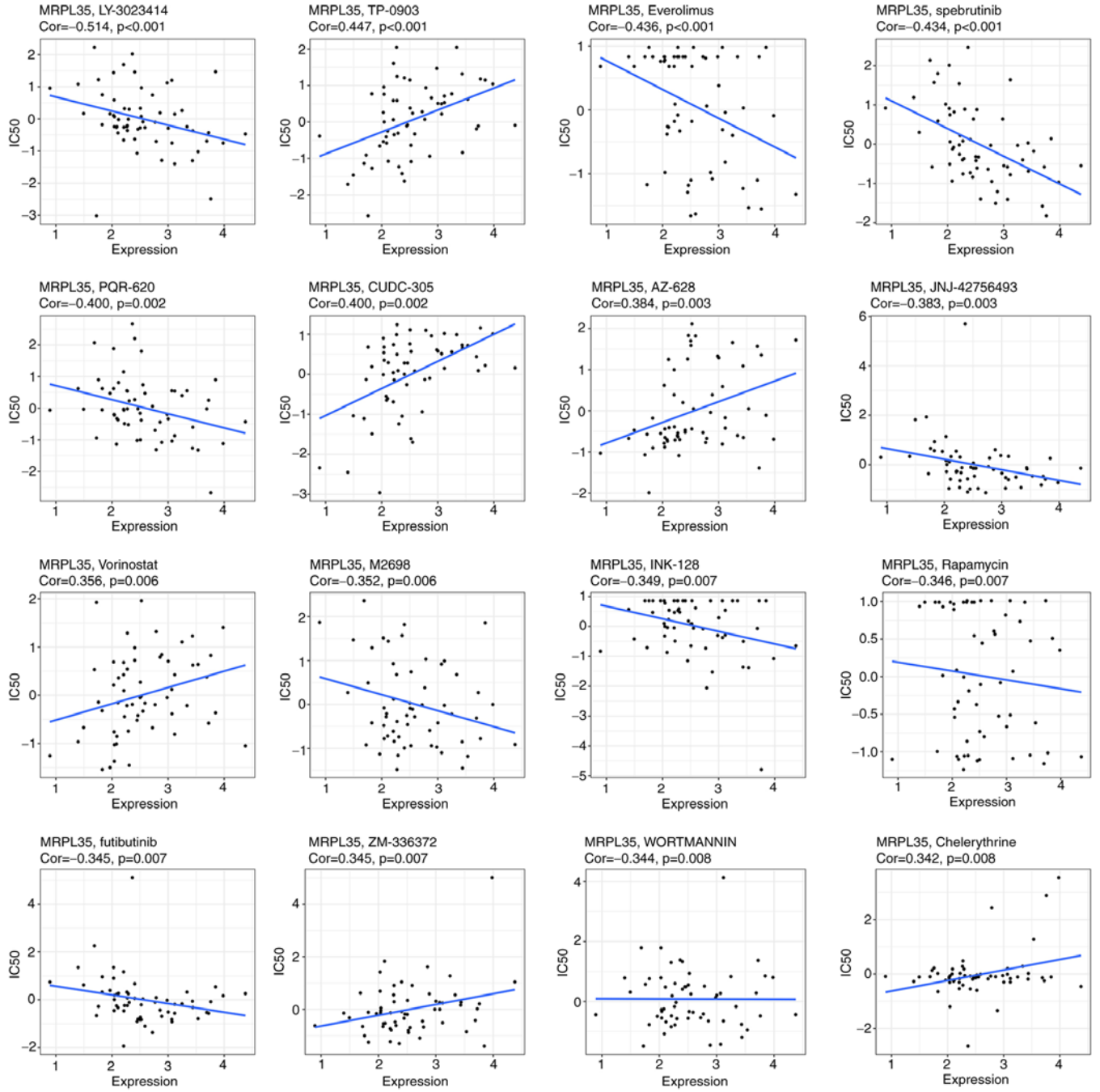

Figure 8. Correlation between the IC_{50} of drugs and MRPL35 level. IC_{50}, half maximal inhibitory concentration; MRPL35, mitochondrial ribosomal protein L35.

this, the group with high WF scores, calculated for the three genes, showed significantly worse outcomes compared with those with low WF scores. Moreover, a relatively repressed immune function was observed in the low WF group, with lower infiltration of $CD8^+$ cells and higher infiltration of M0 macrophages and dendritic resting cells. The relationship between FA metabolism and dysfunctional immunity has been comprehensively reported by Zhang *et al* (38), who indicated that in breast cancer, obesity remodeled the tumor immune microenvironment by promoting the migration of $CD8^+$ T cells through a metabolic shift, thereby suppressing immunity. This metabolic shift was characterized by enhanced FA signaling, leading to STAT3 activation and the subsequent promotion of FA β oxidation and concurrent inhibition of glycolysis due to glucose deprivation. As a result, the ability of $CD8^+$ T cells to restrict tumor proliferation was impaired. In further investigation of the downstream mechanisms in the present study, the results of GSEA indicated that in the high WF group, the TGF-β, hypoxia and IL6/JAK/STAT3 pathways were significantly activated. The activation of each of these signaling pathways has been considered as a strong etiology for tumor development and immune escape in previous studies (39-41); notably, the IL6/JAK/STAT3 signaling pathway has been reported to contribute to immunotherapy resistance (42). These results concur with the conclusions of Fang *et al* (43), Povero *et al* (44) and Zhang *et al* (38). Furthermore, regarding

tumor growth, the KRAS, G2M checkpoint and EMT pathways, which contribute to tumor development and metastasis, were also found to be activated in the high WF score group. Consequently, exploration of the dysregulation of FA metabolism-related genes in HCC has high predictive and therapeutic value.

Due to MRPL35 having the highest HR value among the three genes obtained by the LASSO model, it was chosen for further bioinformatic analysis and validation experiments. The upregulation of MRPL35 at the mRNA and protein levels was observed in cancerous samples compared with normal tissues and in tumors with metastatic status. Since studies have confirmed that methylation of the promoter region of a gene can lead to oncogene activation and the advancement of tumors (45,46), the promoter methylation level of MRPL35 was compared between normal and tumor samples, which showed a significantly lower promoter methylation level in tumors. A relatively high MRPL35 was also be observed in patients with residual tumor status R1 and in female patients, which is of value for clinical guidance. scRNA-seq analysis further confirmed that MRPL35 expression was located in tumor and proliferating T cells. With regard to the immune microenvironment, MRPL35 was found to have a negative correlation with $CD8^+$ T cells and a positive correlation with MDSCs, suggesting the dysfunctional immunity in the high WF score group was probably induced via MRPL35-related pathways. Similarly, Yuan *et al* (34) found that in gastric carcinoma the knockdown of MRPL35 inhibited cell proliferation and colony formation, and induced apoptosis. Furthermore, Zhang *et al* (35) and Alshabi *et al* (47) proposed that MRPL35 plays a promotive role in colorectal cancer and glioblastoma. The present analysis investigated MRPL35-related functions in HCC, which indicated that tumors with a high level of MRPL35 may activate the energy supply process.

In vitro experiments were performed to verify the promotive role of MRPL35 in liver cancer cell migration and invasion, which indicated that after MRPL35 knockdown, these abilities of HepG2 cells were significantly impaired. These results not only confirm the risk role of MRPL35 in metastasis but also support the potential value of MRPL35 as a therapeutic target.

Although the association between the dysregulation of genes associated with FA metabolism was analyzed and validated with *in vitro* experiments, this study has several limitations. First, despite bioinformatics analysis providing a preliminary insight into the crucial role of MRPL35 in HCC progression and drug resistance, future biological experiments *in vivo* are necessary to explore this further. Secondly, the exploration of MRPL35 role in special isotypes of patients also needs conducted, such as patients with certain genetic mutation and with resistance to target/immunotherapy drugs.

In conclusion, the present study uncovered the predictive and therapeutic value of FA metabolism genes in HCC and suggests the potential of targeting these genes to prevent tumor initiation, progression and resistance to drugs.

Acknowledgements

Not applicable.

Funding

No funding was received.

Availability of data and materials

The datasets used and/or analyzed during the current study are available from the corresponding author on reasonable request.

Authors' contributions

ZZ, JS, LW and GT were responsible for study conception and design. JS and LW developed the methodology. LW and ZZ performed data collection. JS, LZ and CJ analyzed and interpreted the data. ZZ and JS wrote, reviewed and revised the manuscript. GT and LW confirm the authenticity of all the raw data. All authors have read and approved the final manuscript.

Ethics approval and consent to participate

Not applicable.

Patient consent for publication

Not applicable.

Competing interests

The authors declare that they have no competing interests.

References

1. Siegel RL, Miller KD and Jemal A: Cancer statistics, 2019. CA Cancer J Clin 69: 7-34, 2019.
2. Allemani C, Matsuda T, Di Carlo V, Harewood R, Matz M, Nikšić M, Bonaventure A, Valkov M, Johnson CJ, Estève J, *et al*: Global surveillance of trends in cancer survival 2000-14 (CONCORD-3): Analysis of individual records for 37 513 025 patients diagnosed with one of 18 cancers from 322 population-based registries in 71 countries. Lancet 391: 1023-1075, 2018.
3. Reig M, Forner A, Rimola J, Ferrer-Fàbrega J, Burrel M, Garcia-Criado Á, Kelley RK, Galle PR, Mazzaferro V, Salem R, *et al*: BCLC strategy for prognosis prediction and treatment recommendation: The 2022 update. J Hepatol 76: 681-693, 2022.
4. Swinnen JV, Brusselmans K and Verhoeven G: Increased lipogenesis in cancer cells: New players, novel targets. Curr Opin Clin Nutr Metab Care 9: 358-365, 2006.
5. Santos CR and Schulze A: Lipid metabolism in cancer. FEBS J 279: 2610-2623, 2012.
6. Medes G, Thomas A and Weinhouse S: Metabolism of neoplastic tissue. IV. A study of lipid synthesis in neoplastic tissue slices in vitro. Cancer Res 13: 27-29, 1953.
7. Alannan M, Fayyad-Kazan H, Trézéguet V and Merched A: Targeting lipid metabolism in liver cancer. Biochemistry 59: 3951-3964, 2020.
8. Budhu A, Roessler S, Zhao X, Yu Z, Forgues M, Ji J, Karoly E, Qin LX, Ye QH, Jia HL, *et al*: Integrated metabolite and gene expression profiles identify lipid biomarkers associated with progression of hepatocellular carcinoma and patient outcomes. Gastroenterology 144: 1066-1075.e1, 2013.
9. Sangineto M, Villani R, Cavallone F, Romano A, Loizzi D and Serviddio G: Lipid metabolism in development and progression of hepatocellular carcinoma. Cancers (Basel) 12: 1419, 2020.
10. Kumagai S, Togashi Y, Kamada T, Sugiyama E, Nishinakamura H, Takeuchi Y, Vitaly K, Itahashi K, Maeda Y, Matsui S, *et al*: The PD-1 expression balance between effector and regulatory T cells predicts the clinical efficacy of PD-1 blockade therapies. Nat Immunol 21: 1346-1358, 2020.

11. Zhou L, Xia S, Liu Y, Ji Q, Li L, Gao X, Guo X, Yi X and Chen F: A lipid metabolism-based prognostic risk model for HBV-related hepatocellular carcinoma. Lipids Health Dis 22: 46, 2023.
12. Feng T, Wu T, Zhang Y, Zhou L, Liu S, Li L, Li M, Hu E, Wang Q, Fu X, *et al*: Stemness analysis uncovers that the peroxisome proliferator-activated receptor signaling pathway can mediate fatty acid homeostasis in sorafenib-resistant hepatocellular carcinoma cells. Front Oncol 12: 912694, 2022.
13. Bensaad K, Favaro E, Lewis CA, Peck B, Lord S, Collins JM, Pinnick KE, Wigfield S, Buffa FM, Li JL, *et al*: Fatty acid uptake and lipid storage induced by HIF-1α contribute to cell growth and survival after hypoxia-reoxygenation. Cell Rep 9: 349-365, 2014.
14. Murai H, Kodama T, Maesaka K, Tange S, Motooka D, Suzuki Y, Shigematsu Y, Inamura K, Mise Y, Saiura A, *et al*: Multiomics identifies the link between intratumor steatosis and the exhausted tumor immune microenvironment in hepatocellular carcinoma. Hepatology 77: 77-91, 2023.
15. Gualdoni GA, Mayer KA, Göschl L, Boucheron N, Ellmeier W and Zlabinger GJ: The AMP analog AICAR modulates the Treg/Th17 axis through enhancement of fatty acid oxidation. FASEB J 30: 3800-3809, 2016.
16. Chen L, Zhou Q, Liu J and Zhang W: CTNNB1 alternation is a potential biomarker for immunotherapy prognosis in patients with hepatocellular carcinoma. Front Immunol 12: 759565, 2021.
17. Shen S, Khatiwada S, Behary J, Kim R and Zekry A: Modulation of the gut microbiome to improve clinical outcomes in hepatocellular carcinoma. Cancers (Basel) 14: 2099, 2022.
18. Goldman MJ, Craft B, Hastie M, Repečka K, McDade F, Kamath A, Banerjee A, Luo Y, Rogers D, Brooks AN, *et al*: Visualizing and interpreting cancer genomics data via the Xena platform. Nat Biotechnol 38: 675-678, 2020.
19. Subramanian A, Tamayo P, Mootha VK, Mukherjee S, Ebert BL, Gillette MA, Paulovich A, Pomeroy SL, Golub TR, Lander ES and Mesirov JP: Gene set enrichment analysis: A knowledge-based approach for interpreting genome-wide expression profiles. Proc Natl Acad Sci USA 102: 15545-15550, 2005.
20. Mootha VK, Lindgren CM, Eriksson KF, Subramanian A, Sihag S, Lehar J, Puigserver P, Carlsson E, Ridderstråle M, Laurila E, *et al*: PGC-1alpha-responsive genes involved in oxidative phosphorylation are coordinately downregulated in human diabetes. Nat Genet 34: 267-273, 2003.
21. Bartha Á and Győrffy B: TNMplot.com: A web tool for the comparison of gene expression in normal, tumor and metastatic tissues. Int J Mol Sci 22: 2622, 2021.
22. Langfelder P and Horvath S: WGCNA: An R package for weighted correlation network analysis. BMC Bioinformatics 9: 559, 2008.
23. Ranstam J and Cook JA: Statistical nugget LASSO regression. Br J Surg 105: 1348, 2018.
24. Vasaikar SV, Straub P, Wang J and Zhang B: LinkedOmics: Analyzing multi-omics data within and across 32 cancer types. Nucleic Acids Res 46 (D1): D956-D963, 2018.
25. Shen W, Song Z, Zhong X, Huang M, Shen D, Gao P, Qian X, Wang M, He X, Wang T, *et al*: Sangerbox: A comprehensive, interaction-friendly clinical bioinformatics analysis platform. iMeta 1: e36, 2022.
26. Newman AM, Liu CL, Green MR, Gentles AJ, Feng W, Xu Y, Hoang CD, Diehn M and Alizadeh AA: Robust enumeration of cell subsets from tissue expression profiles. Nat Methods 12: 453-457, 2015.
27. Li T, Fu J, Zeng Z, Cohen D, Li J, Chen Q, Li B and Liu XS: TIMER2.0 for analysis of tumor-infiltrating immune cells. Nucleic Acids Res 48 (W1): W509-W514, 2020.
28. Sun D, Wang J, Han Y, Dong X, Ge J, Zheng R, Shi X, Wang B, Li Z, Ren P, *et al*: TISCH: A comprehensive web resource enabling interactive single-cell transcriptome visualization of tumor microenvironment. Nucleic Acids Res 49 (D1): D1420-D1430, 2021.
29. Livak KJ and Schmittgen TD: Analysis of relative gene expression data using real-time quantitative PCR and the 2(-Delta Delta C(T)) method. Methods 25: 402-408, 2001.
30. Reinhold WC, Sunshine M, Liu H, Varma S, Kohn KW, Morris J, Doroshow J and Pommier Y: CellMiner: A web-based suite of genomic and pharmacologic tools to explore transcript and drug patterns in the NCI-60 cell line set. Cancer Res 72: 3499-3511, 2012.
31. Jeon YG, Kim YY, Lee G and Kim JB: Physiological and pathological roles of lipogenesis. Nat Metab 5: 735-759, 2023.
32. Lin L, Wen J, Lin B, Chen H, Bhandari A, Qi Y, Zheng D and Wang O: Phospholipase C Delta 3 inhibits apoptosis and promotes proliferation, migration, and invasion of thyroid cancer cells via Hippo pathway. Acta Biochim Biophys Sin (Shanghai) 53: 481-491, 2021.
33. Hu H, Yin Y, Jiang B, Feng Z, Cai T and Wu S: Cuproptosis signature and PLCD3 predicts immune infiltration and drug responses in osteosarcoma. Front Oncol 13: 1156455, 2023.
34. Yuan L, Li JX, Yang Y, Chen Y, Ma TT, Liang S, Bu Y, Yu L and Nan Y: Depletion of MRPL35 inhibits gastric carcinoma cell proliferation by regulating downstream signaling proteins. World J Gastroenterol 27: 1785-1804, 2021.
35. Zhang L, Lu P, Yan L, Yang L, Wang Y, Chen J, Dai J, Li Y, Kang Z, Bai T, *et al*: MRPL35 is up-regulated in colorectal cancer and regulates colorectal cancer cell growth and apoptosis. Am J Pathol 189: 1105-1120, 2019.
36. Aiyappa-Maudsley R, Storr SJ, Rakha EA, Green AR, Ellis IO and Martin SG: CYP2S1 and CYP2W1 expression is associated with patient survival in breast cancer. J Pathol Clin Res 8: 550-566, 2022.
37. Guo H, Zeng B, Wang L, Ge C, Zuo X, Li Y, Ding W, Deng L, Zhang J, Qian X, *et al*: Knockdown CYP2S1 inhibits lung cancer cells proliferation and migration. Cancer Biomark 32: 531-539, 2021.
38. Zhang C, Yue C, Herrmann A, Song J, Egelston C, Wang T, Zhang Z, Li W, Lee H, Aftabizadeh M, *et al*: STAT3 activation-induced fatty acid oxidation in $CD8^+$ T effector cells is critical for obesity-promoted breast tumor growth. Cell Metab 31: 148-161.e5, 2020.
39. Datta J, Dai X, Bianchi A, De Castro Silva I, Mehra S, Garrido VT, Lamichhane P, Singh SP, Zhou Z, Dosch AR, *et al*: Combined MEK and STAT3 inhibition uncovers stromal plasticity by enriching for cancer-associated fibroblasts with mesenchymal stem cell-like features to overcome immunotherapy resistance in pancreatic cancer. Gastroenterology 163: 1593-1612, 2022.
40. Xie F, Zhou X, Su P, Li H, Tu Y, Du J, Pan C, Wei X, Zheng M, Jin K, *et al*: Breast cancer cell-derived extracellular vesicles promote $CD8^+$ T cell exhaustion via TGF-β type II receptor signaling. Nat Commun 13: 4461, 2022.
41. Bourayou E and Golub R: Signaling pathways tuning innate lymphoid cell response to hepatocellular carcinoma. Front Immunol 13: 846923, 2022.
42. Johnson DE, O'Keefe RA and Grandis JR: Targeting the IL-6/JAK/STAT3 signalling axis in cancer. Nat Rev Clin Oncol 15: 234-248, 2018.
43. Fang Y, Zhang Q, Lv C, Guo Y, He Y, Guo P, Wei Z, Xia Y and Dai Y: Mitochondrial fusion induced by transforming growth factor-β1 serves as a switch that governs the metabolic reprogramming during differentiation of regulatory T cells. Redox Biol 62: 102709, 2023.
44. Povero D, Chen Y, Johnson SM, McMahon CE, Pan M, Bao H, Petterson XT, Blake E, Lauer KP, O'Brien DR, *et al*: HILPDA promotes NASH-driven HCC development by restraining intracellular fatty acid flux in hypoxia. J Hepatol 79: 378-393, 2023.
45. Piao GH, Piao WH, He Y, Zhang HH, Wang GQ and Piao Z: Hyper-methylation of RIZ1 tumor suppressor gene is involved in the early tumorigenesis of hepatocellular carcinoma. Histol Histopathol 23: 1171-1175, 2008.
46. Chen G, Fan X, Li Y, He L, Wang S, Dai Y, Bin C, Zhou D and Lin H: Promoter aberrant methylation status of ADRA1A is associated with hepatocellular carcinoma. Epigenetics 15: 684-701, 2020.
47. Alshabi AM, Vastrad B, Shaikh IA and Vastrad C: Identification of crucial candidate genes and pathways in glioblastoma multiform by bioinformatics analysis. Biomolecules 9: 201, 2019.